The X-ray Absorption Spectra of AGNs

T. Kallman

Laboratory for High Energy Astrophysics, NASA/GSFC

Abstract. X-ray absorption provides important clues to the origins of the gas flows in active galaxies and quasars (AGN). Both observational and theoretical evidence suggests that a large fraction of the gas in these objects is highly ionized, and therefore best observed in X-rays. Current X-ray spectral observations constrain the degree of ionization of this gas. I will present a summary of these results, together with a discussion of models for the spectra and predictions for future observations.

1. Background

The optical and ultraviolet (UV) spectra of quasars and active galactic nuclei (AGN) are characterized by strong, broad emission lines covering a wide range of ionization. The apparent similarity of the profiles of these various lines in early, low-resolution spectra (Baldwin 1975) led to the suggestion that they originate in the same gas: the broad emission line region (BLR). Since then much effort has been directed towards understanding the generation of these lines and the physical conditions in the BLR gas, leading to the development of the standard photoionization model. The ultimate goal of such studies is to understand the quasar energy source: the mass, size, and fueling mechanism. Line spectra can help with this determination by providing constraints on the gas velocities, ionization balance, column density and elemental abundance. Over the years various dynamical models have been proposed to account for the broad lines, although there is no consensus so far on which of these best accounts for the properties of broad emssion lines. It is likely that the gas seen in the UV is accompanied by a comparable or greater mass of gas which is hot and highly ionized, and which is best studied in the X-ray band. The various dynamical scenarios do, in fact, make distinct predictions concerning the X-ray spectra, and these differences and the prospects for detecting them are the subject of this paper.

The standard BLR model (as described, e.g. in Davidson and Netzer 1979, Kwan and Krolik, 1981; Weisheit Shields and Tarter, 1982) postulates that AGN emission lines arise in a large number of small clouds, all having very similar physical conditions, which surround a central compact source of continuum radiation. The heating and photoionization produced by this continuum is, in this model, the dominant mechanism contributing to line emission. This view has had significant success in accounting for several gross properties of AGN spectra, including the broad line equivalent widths, the absence (or at least rarity) of hydrogen continuum absorption, and most notably, the flux ratios of the UV emission lines. Problems of detail prevent complete acceptance of this model, however. For example, the L α/ Hβ ratio, observed to be ~ 5 (Baldwin 1977), is a factor of several smaller than in any suggested model (Ferland and Mushotzky 1984, Collin-Souffrin and Dumont 1986, Kallman and Krolik 1986); and the large (and uncertain) strength of the FeII lines (Wills, Netzer and Wills 1985) has yet to find an adequate heat source. Most seriously, the quality of data available from recent variability studies (e.g. Korista et al. 1995, Krolik et al., 1991) has undercut the earlier satisfaction with single-zone models for the physical conditions in the BLR.

In fact, as a result of the recent variability campaigns, the first elements of a multi-zone picture of the broad emission line region have begun to emerge. An essential part of that picture is the evidence that line-emitting material generally exists over a wide range of distances from the central object (see, for example, Krolik et al. 1991, and Rees, Netzer and Ferland, 1989, and Netzer, 1987). This has provided further impetus for the quest for a dynamical model for the BLR gas.

In this paper we discuss several simple dynamical models and the predictions they make concerning hot gas which is potentially observable in the X-ray band. Any effort in this area is hampered by the fact that all available dynamical models are either greatly simplified, and therefore incomplete, or make predictions which are discrepant with some aspects of the AGN database (such as the data from variability campaigns). Nevertheless, they represent the best that can be done based on current work, and the qualitative predictions are likely to hold even when the models have been worked out in more detail. Furthermore, significant improvements in the available X-ray instrumentation are imminent (AXAF, XMM, Astro-E), which add impetus to consideration of these models. In section 2 we begin by describing the constraints imposed on all models by the photoionization models for the broad lines. In section 3 we briefly describe each of 4 dynamical models and their predictions for the conditions in the hot gas. In section 4 we provide synthetic X-ray spectra illustrating some possible differences between the model predictions, and in section 5 we examine the prospects for observational detection of these features.

2. Standard BLR Parameters (inferred from UV emission lines)

According to standard photoionization model arguments, the broad emission lines are emitted from a large number of clouds surrounding a central compact object. The clouds are heated and ionized by the continuum radiation from the central object, and cool primarily via line emission. The lines are broadened by the cloud velocities, which can exceed 10^4 km s^{-1}. The arguments leading up to this scenario have been reviewed by Davidson and Netzer (1979) and references therein. In the most general case the clouds may have a distribution of velocities and sizes at any point within the region, and the cloud number density distribution may have a complicated dependence on position within the region. The line emission properties depend on the shape of the ionizing continuum, the gas elemental composition, the gas pressure, and on the ratio of the radiation flux to the gas pressure or density (the 'ionization parameter'). In what follows we use both

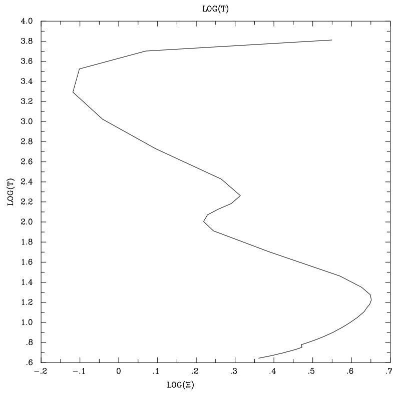

Figure 1. Temperature of photoionized gas (in units of 10^4 K) as a function of ionization parameter, logΞ. Ionizing spectrum is a single power law with energy index 1.

the definition $\Xi = L/(4\pi R^2 cP)$ (Krolik, McKee, and Tarter, 1981) and $\xi = L/(nR^2)$, where L is the ionizing luminosity in energy units, R is the distance from the continuum source, P is the gas pressure, and n is the gas density.

In order to fit the observed line strengths, the UV line emitting gas in the BLR must have the following approximate values: ionization parameter $\log(\Xi_{UV}) = -1 - 10$, gas density $n_{UV} = 10^{10} - 10^{12}$ cm^{-3}, gas temperature: $T_{UV} \simeq 10^4$ K, gas pressure: $P_{UV} = 0.01 - 1.$ dyne cm^{-2} s^{-1}, mean distance from the central source $R_{UV} = 1.6 \times 10^{16} L_{44}^{1/2} P^{-1/2} \Xi^{-1/2}$, and column density $N_{UV} = 10^{22} - 10^{23}$ cm^{-2}.

3. Dynamical Models

3.1. Model 1: Spherical Infall

This model is the simplest model for BLR gas, and it is included here primarily for the purposes of comparison with more detailed models. According to this model the UV emitting gas is in the form of clouds or filaments, each conforming approximately to the properties described in the previous section. The gas is on its way to being accreted by the central source, and so is falling into the central source with a freefall velocity (Krolik and London, 1981; Kallman, et al., 1993; Kwan and Carroll, 1982). If so, the accretion rate must be sub-Eddington in order to avoid the influence of radiation pressure, and the accretion efficiency (η) must be low ($\leq 10^{-3}$) in order to avoid complete ionization of the UV emitting gas. A requirement is that the UV emitting gas must be confined by a hot ($\sim 10^7$K), tenuous, intercloud medium (ICM) in order to avoid cloud dispersal on a free expansion timescale (Krolik, McKee, and Tarter, 1981). This ICM can coexist at the same ionization parameter as with UV emitting gas owing to the thermal properties of photoionized gas in the presence of Compton heating, as illustrated in Figure 1. The properties of this hot gas are as follows: temperature $T \simeq 10^7$ K, pressure $P \simeq P_{UV}$, ionization parameter $\Xi_h^* \leq \Xi \leq \Xi_c^*$, where $\xi = \Xi 4\pi ckT = 5.4 \times 10^2 \Xi T_7$. Ξ_h^* and Ξ_c^* are the bounding values of the 2 phase region shown in figure 1. The gas density is $n = P/kT = 7.2 \times 10^8 P/T_7$cm^{-3} $= n_{ICM}$, radius $R = R_{UV}$, and column density: $N = nR = 7.2 \times 10^{24} P R_{16}/T_7$ cm^{-2}.

3.2. Model 2: Star cluster

The spherical infall model has shortcomings which include the large masses for AGN central objects implied by the low efficiency, and which are not confirmed by other dynamical arguments, and the unknown origin for the filamentary clouds. A potential solution to some of these problems is that the UV emitting gas originates in the atmospheres of stars (e.g. Alexander and Netzer, 1997, Kazanas, 1988; Penston, 1988). If so, the accretion efficiencies and Eddington ratios may be close to unity. An unavoidable consequence of this model is that the stars will shed gas, which will produce an ICM, owing to the combined effects of X-ray evaporation, ordinary mass loss, and stellar collisions and tidal disruption. A lower limit to the ICM density is obtained by assuming that the evaporative rate from the stars themselves is balanced by a hot wind which removes the gas from the BLR.

The mass loss rate due to evaporation from one star can be estimated as (c.f. Begelman, McKee and Shields, 1982; London, McCray, and Auer, 1981): $\dot{M} \simeq \pi R_*^2 \left(\frac{P_{min}}{kT}\right) m_H c_s$. The mass loss rate in the evaporative flow from an ensemble of stars can be written in terms of the covering fraction C as $\dot{M} = C\left(\frac{L}{4cc_s\Xi}\right) = 0.05 M_\odot \mathrm{yr}^{-1} L_{44} C_{0.1} T_7^{-1} \Xi^{-1}$, where c_s is the sound speed. The mass loss rate from the BLR due to an evaporative wind is: $\dot{M} = \frac{L}{ckT\Xi} c_s m_H$. Balancing the two $\dot{M}$ expressions gives the mean ICM ionization parameter: $\Xi = \Xi_c^* \frac{4}{C} \simeq 40 \Xi_c^*$; $\xi = 2.2 \times 10^4 T_7 \Xi_c^*$. The mean density and column density are $n = \left(\frac{L}{4\pi R^2 ckT\Xi}\right) = n_{ICM} \frac{\Xi_c^*}{\Xi} = \frac{n_{ICM}}{40}$ and $N = nR = 1.8 \times 10^{23} P R_{16}/T_7$ cm^{-2}. So, compared with model 1, the wind serves to clean out some of the hot gas in the BLR resulting in a higher ionization parameter and lower column density.

3.3. Model 3: Radiation Pressure Driven Disk Wind

An alternative origin for BLR material is that it originates in a wind from the surface of an accretion disk. A possible wind driving mechanism is radiation pressure from the disk photosphere acting on the UV resonance lines in a manner equivalent to that known to drive winds from the atmospheres of hot stars (e.g. Murray et al., 1994; Shlosman et al., 1985). If so, a constraint on the wind mass loss rate and density comes from the total momentum flux available from the disk photospheric radiation. The wind density turns out to be $n \simeq \frac{3}{8\pi} \frac{\dot{M}_{acc}}{R^2 c m_H} \frac{4\pi}{\Omega} = 10^5 \frac{4\pi}{\Omega} L_{44} R_{16}^{-2} \eta_{0.1}^{-1}$, where $\Omega/4\pi$ is the fractional solid angle subtended by the wind. The ionization parameter is $\xi = 10^7 \frac{\Omega}{4\pi} \eta_{0.1}$. The column density is: $N = nR = 10^{22} \frac{4\pi}{\Omega} L_{44} R_{16}^{-1} \eta_{0.1}^{-1}$. Owing to the very large ionization parameter, the UV emitting gas must be shielded from the full intensity of the ionizing radiation. In order to make the column density high enough we require $\frac{\Omega}{4\pi} \sim 0.01$. This results in a column $N \sim 10^{24}$ cm^{-2} and $\xi \sim 10^4$ for lines of sight which pass through the hot gas.

3.4. Model 4: Magnetohydrodynamic Disk Wind[4]

The line driven disk wind has severe constraints on mass loss imposed by the momentum conservation condition. The only way that these can allow for the existence of gas capable of emitting UV lines is if the gas is compressed into a relatively small solid angle, as shown in the previous subsection. The constraints on the mass loss rate in a disk wind are removed if it is driven by another mechanism. One possibility is magnetic pressure

(Bottorf, et al., 1997; Blandford and Payne, 1982). If so, density, ionization parameter and column density are: $n \simeq n_{UV} = 10^{10} n_{10} \mathrm{cm}^{-3}$, $\xi = 10^2 L_{44} R_{16}^{-2} n_{10}^{-1} \mathrm{ergcms}^{-1}$, $N = nR = 10^{26} n_{10} R_{16} \mathrm{cm}^{-2}$.

4. Simulations

In order to illustrate the possible signatures expected from hot gas in AGNs we show in figure 2 a set of synthetic spectra. These are calculated by assuming photoionization equilibrium and a constant value of ionization parameter and column density. The ionization parameter in this case is described by ξ, adopting the definition given above.

Any calculation of synthetic spectra must inevitably make some assumption about the geometry of the BLR gas. Even though this is, in principle, prescribed by the dynamical models, it is instructive to consider the general properties of various geometries, which we denote by the terms spherical, prolate and oblate. In doing so, we can distinguish between the various processes occuring in the gas as either scattering (i.e. elastic) or absorption followed by reemission (or inelastic scattering). Electron scattering and resonance line scattering are examples of the former, while continuum photoabsorption followed by recombination are examples of the latter. If, for example, the geometry of the BLR gas is spherical, and if the gas is stationary, then the scattering processes result in no net change to the emergent X-ray spectrum, while the inelastic processes result in a redistribution of photons in energy and creation of absorption troughs and recombination continuum emission features. Any net motion of a spherical BLR will results in P-Cygni (or inverse P-Cygni) profiles in the resonance lines. If the BLR is non-spherical, say a cone or wedge of gas oriented along the observer's line of sight (prolate), then absorption will predominate over scattered or recombination emission, both for lines and for continua. The converse applies if the non-spherical structure is not oriented toward the observer (oblate).

The present simulations are motivated by the observational fact that, in the X-ray spectral band, absorption troughs associated with known photoelectric edges from ions such as O VII and O VIII are observed from many low luminosity AGN (e.g. George, et al., 1997), while the corresponding recombination continuum emission features are not unambiguosly detected in as many objects. Resonance line emission from ions associated with these edges also has not been clearly detected. Although both lines and recombination continuum emission features are likely to be narrow compared with the spectral resolution of current X-ray instruments, such as *ASCA*, the available evidence suggests that for many objects the prolate scenario is most appropriate.

The spectra shown in Figure 3 assume pure absorption for both resonance lines and photoelectric abosrption. The procedure and atomic dataset are the same as those used in Kallman et al. (1996), and the lines are assumed to have a width corresponding to a gas velocity of 1000 km/s. We feel that this is appropriate given the broadening of the UV lines, both in emission and in absorption. The resolution used in binning the lines in this figure corresponds to this velocity.

These figures illustrate the range of spectra which may be produced by hot gas associated with the BLR, and the dependence of the spectra on the free parameters of the model, the column density and ionzation parameter. The mean ionization state of a photoionized gas is proportional to the ionization parameter. At high ionization

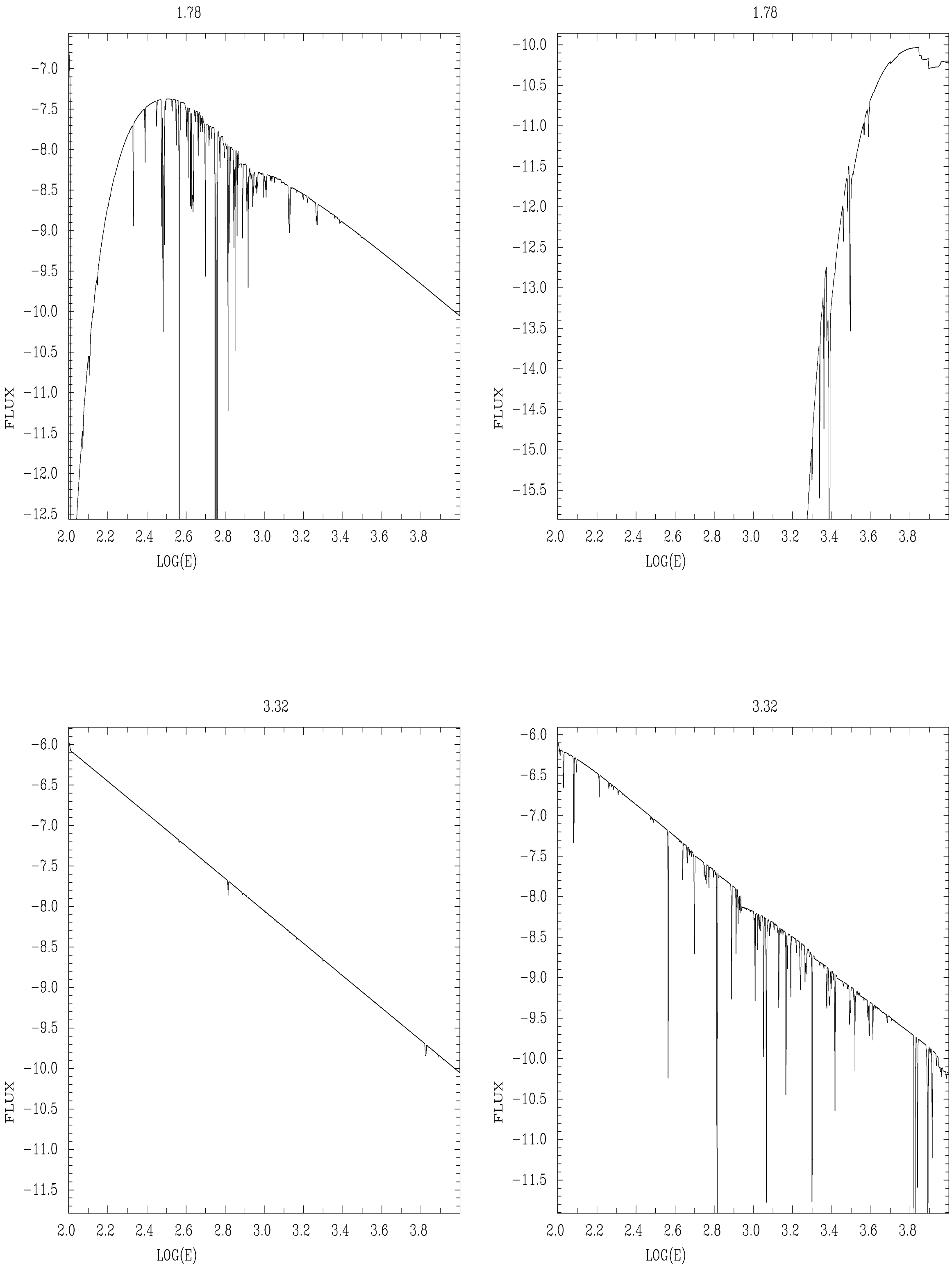

Figure 2. Sample synthetic spectra from AGN warm absorber gas. Frames are labelled with the ionization papameter value ($\log(\xi)$). Left frames have column 10^{22} cm^{-2}, right panels have column 10^{24} cm^{-2}.

parameter the ions with the greatest fractional abundance belong to material of relatively high nuclear charge, Z. Owing to the lower abundance and lower photoionization cross sections associated with higher Z, a greater column density of gas is required in order to produce significant absorption. Thus there is an approximate proportionality between ionization parameter and this critical column density. Figure 2 shows that a column density of 10^{22} cm^{-2} produces greater absorption at $\log(\xi)$=1.78 than at $\log(\xi)$=3.32.

The potential importance of lines in these spectra was first pointed out by Krolik and Kriss (1995) and by Kriss et al. (1996). Quantitive measures of the importance of lines depend on many details of the modelling and measurement criteria, including the intrinsic broadening assumed, the resolution used to measure the line strengths, the elemental abundances assumed, the atomic dataset employed for the modelling, and assumptions concerning the excitation level in the gas. In the following section some of these issues are addressed in more detail. As we will demonstrate, the net equivalent width of the line absorption is less than that of the continuum.

From Figure 2 we can crudely predict the spectra which may correspond to the various dynamical models. It is convenient to compare them pairwise: model 2 has greater ionization parameter and lower column density than model 1, and models 3 and 4 have an analagous relationship. Model 4 is expected to produce an absorption spectrum resembling that shown in the upper left of Figure 2, and model 2 is expected to resemble that shown in the lower right of Figure 2. The other 2 models would produce spectra with intermediate properties. Although these results are based on highly simplified estimates of the model properties, and the synthetic spectra are idealized, single zone models, the general relationships of the model predictions relative to each other and the qualitative appearance of the synthetic spectra are straightforward and relatively secure.

5. Observability

As stated in the previous section, it is difficult to evaluate the importance of X-ray absorption without some quantitative criterion. We have attempted to construct such a criterion by analyzing our synthetic spectra in the following way. For each spectrum in a grid of models consisting of a 20 x 20 grid of ionization parameter and column density, we assume that the spectrum is observed by a fictitious instrument with a given effective area, resolving power, and observing time. We convolve the model with a simplified (diagonal) response matrix for this instrument and add (Gaussian) counting statistics in order to produce a fake observed count spectrum. We then calculate the χ^2 between this fake spectrum and that produced by the model without counting statistics. We use 3 trial models: (i) the full model used in creating the fake count spectrum (i.e. equivalent to those shown in Figure 2); (ii) the same as (i) but with the resonance line component artificially removed; and (iii) a pure power law with no absorption at all. A measure of the significance of the absorption is then obtained by comparing the χ^2 produced by each trial spectrum. If χ^2_i is the χ^2 produced by model (i), χ^2_{ii} is the χ^2 produced by model (ii),etc., we define $\Delta\chi^2_{i,ii} = \chi^2_{ii} - \chi^2_i$ $\Delta\chi^2_{i,iii} = \chi^2_{iii} - \chi^2_i$. When $\Delta\chi^2_{i,iii} \geq 10$, say, we consider the continuum photoabsorption to have been detected, and when $\Delta\chi^2_{i,ii} \geq 10$ we consider the resonance lines to have been detected.

In choosing our fictitious instruments we consider 3 different combinations: (a) A=200 cm^2, R=20, t_{obs}=10 second, (b) A=200 cm^2, R=20, t_{obs}=10^5 second, and (c) observation (a)

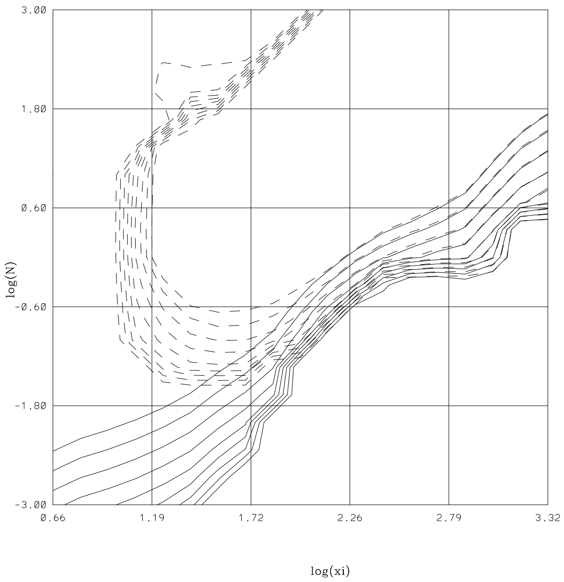

observation (b)

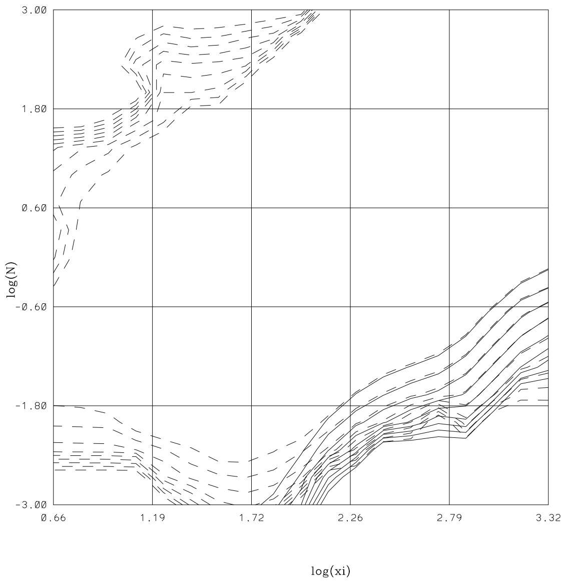

observation (c)

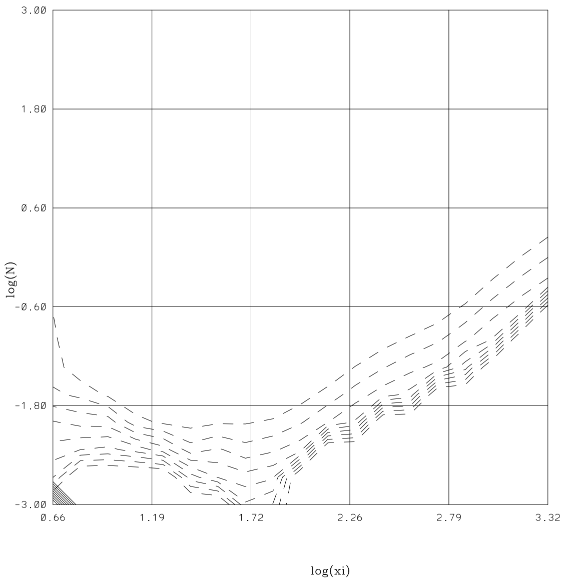

observation (d)

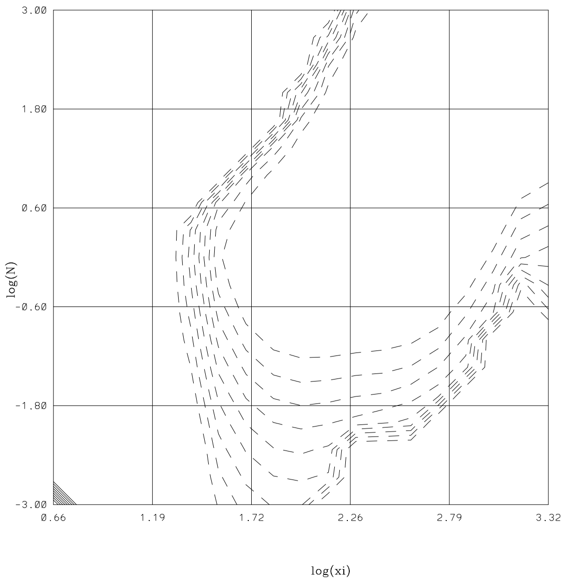

A=200 cm^2, R=600, t_{obs}=10^5 second. All these assume line broadening of 1000 km s^{-1}. In addition we consider combination (d), which is the same as (c) but which has purely thermal widths (i.e. 10-50 km s^{-1}) assumed for the lines rather than 1000 km s^{-1}. The normalization of the input spectrum in the absence of absorption is assumed to be 0.01 erg cm^{-2} s^{-1} erg^{-1} at 1 keV, which is comparable to that of relatively bright, low luminosity AGN (e.g. Kriss et al., 1996). The results are shown as contours of constant log($\Delta\chi^2_{i,ii}$) (dashed curves) and log($\Delta\chi^2_{i,iii}$) (solid curves) in figure 3. In this Figure, the horizontal axis is logξ, and the vertical axis is log(N), where the units of N is 10^{22} cm^{-2}. The contours correspond to constant log($\Delta\chi^2$) and are separated by 0.5 dex. Thus, the lower right corner of each panel corresponds to non-detection of any absorption ($\Delta\chi^2 \simeq$ 0). This reflects the fact that at low columns the effects of any absorption are negligible. The boundary separating the region of detection from the region of non-detection of absorption is generally a diagonal band from the lower left part of each diagram to the upper right, reflecting the fact that absorption is most easily detectable, at a given column density, at low ionization parameter when the gas is more nearly neutral.

This band is clearly apparent in the observation (a) panel; for this observation at the lowest columns absorption cannot be unambiguously detected even at the lowest ionization parameters. The boundary of the region of detection of lines is almost congruent with the boundary of the continuum detection region, showing that lines cannot be distinguished from continuum absorption for such an observation. The fact that the line detection region has an approximate 'U' shape in all the panels is a reflection of the fact that lines are undetectable when the gas is very opaque to continuum photoabsorption. Panel (b) shows similar qualitative behavior to panel (a), except that the increased observation time allows detection of absorption over a greater fraction of parameter space. In panels (c) and (d) the continuum abosrption is detectable over virtually the entire parameter space, while line detection requires a column which is greater by at least 0.5 dex.

These results serve to demonstrate the potential for detecting X-ray absorption features, both lines and continua, and for using them to test dynamical models for AGN BLR gas. Such detections have been made using the *ASCA* satellite, which resemble observation (b). This suggests that most AGN have parameters near the lower part of the Figure 3 panels. The AXAF gratings will resemble observations (c) and (d). These will allow detection of lines for observations somewhat longer than those considered here over virtually the entire parameter space, and provide a potential test of various dynamical models.

References

Alexander, T., and Netzer, H., 1997, MNRAS 284, 967

Baldwin, J., 1975; Ap. J.; 201; 26

Baldwin, J., 1977; Ap. J.; 214; 679

Baldwin, J., and Netzer, H., 1978; Ap. J.; 226; 1

Blandford, R., and Payne, D., 1982, MNRAS 199, 883

Bottorf, M., Kroista, K., Shlosman, I., and Blandford, R., 1997, Ap. J., 479, 200

Collin-Souffrin, S., and Dumont, A., 1986; Ast. and Ap.; 166; 13

Davidson, K., and Netzer, H., 1979; Rev. Mod. Phys.;;

Ferland, G., and Mushotzky, R. F., 1982; Ap. J.; 262; 564

Ferland, G., and Netzer, H., 1984; Ap. J.; 264; 105

Ferland, G., Netzer, H., and Shields, G., 1979; Ap. J.; 232; 382

George, I. M.; Turner, T. J.; Netzer, H.; Nandra, K.; Mushotzky, R. F.; Yaqoob, T., 1998, Ap. J., 114, p.73

Kallman, T. R., Liedahl, D., Osterheld, A., Goldstein, W., and Kahn, S., 1996, Ap. J., 465, 994

Kallman, T.R., Wilkes, B., Krolik, J., and Green, R., 1993, Ap.J., 403, 45.

Kallman, T. R.,and Krolik, J. H., 1986; Ap. J.; 308; 805

Kallman, T. R., and Mushotzky, R. F., 1986; Ap. J.; 292; 49

Kazanas, D., 1989, Ap. J., 347, 74

Korista, K., et al., 1995; Ap. J. Supp., 97, 285

Kriss, G. A., et al., 1996, Ap. J., 469, 698

Krolik, J., and Kriss, G., 1995 Ap. J. 447, 512

Krolik, J. H., McKee, C. F., and Tarter, C. B., 1981; Ap. J.; 249; 422

Krolik, J. H., and London, R., 1984; Ap. J.; 267; 18

Krolik, J. H., and Kallman, T. R., 1988; Ap. J.; 324; 714

Krolik, J. H., 1988; Ap. J.; 325; 148

Krolik, J. H., Horne, K., Kallman, T. R.,Kriss, J., and Malkan, M., 1991; Ap. J.; 371; 541

Kwan, J., and Carroll, B., 1982; Ap. J.; 261; 25

Kwan, J., and Krolik, J. H., 1981; Ap. J.; 250; 478

Mathews, W., and Ferland, G., 1987; Ap. J.; 323; 456

Murray, N., Chiang, J., Voit, and Grossman, S., 1994, Ap. J., 451, 498

Netzer, H., 1987; MNRAS; 225; 55

Penston, M., 1988, MNRAS 233 601

Rees, M., Netzer, H., and Ferland, G., 1989; Ap. J.; 347; 640

Shlosman, I., Vitello, P.A., and Shaviv, G., 1985; Ap. J.; 294; 96

Weisheit, J., Shields, G., and Tarter, C. B., 1982; Ap. J.; 245; 406

Wills, B., Netzer, H., and Wills, D., 1985; Ap. J.; 288; 94